Advanced electrokinetic characterization of layer-by-layer assembled polyelectrolyte membranes: Consideration and use of the electrokinetic leakage phenomenon

Agathe Lizée, Penglin Fan, Patrick Loulergue, Anthony Szymczyk

Advanced electrokinetic characterization of layer-by-layer assembled polyelectrolyte membranes: consideration and use of the electrokinetic leakage phenomenon

Agathe Lizée, Penglin Fan, Patrick Loulergue, Anthony Szymczyk*

Univ Rennes, CNRS, ISCR (Institut des Sciences Chimiques de Rennes) – UMR 6226, F-35000 Rennes, France

*corresponding author: anthony.szymczyk@univ-rennes1.fr

Abstract

The sensitivity of zeta potential to the sign of the surface charge of membranes makes it an interesting parameter for the characterization of layer-by-layer (Lbl) modified polyelectrolytes membranes. However, during tangential electrokinetic measurements, a non-negligible parasitic phenomenon referred to as "electrokinetic leakage" may occur. If not taken into account, this phenomenon can lead to dramatic quantitative and qualitative errors, especially when it comes to characterize the surface charge of layer-by-layer assembled polyelectrolyte membranes. In this work, we show that it can lead to substantial errors when interpreting experimental data, including misinterpreting the sign of the membrane surface charge density. An advanced protocol based on the measurement of the streaming current by varying the spacing between the two samples needed for the measurements allows to (i) correct the raw data for the electrokinetic leakage phenomenon and thus to correctly and accurately determine the zeta potential of the membrane surface and (ii) to detect whether polyelectrolytes are deposited only on the membrane surface or whether they can also penetrate into the membrane pores. The approach followed and the conclusions drawn in this study can be straightforwardly applied to any kind of membrane functionalization.

Keywords: Tangential streaming current, zeta potential, electrokinetic leakage, layer-by-layer modification, polyelectrolyte membranes.

1. Introduction

Zeta potential is a widely-used indicator providing insight on materials surface charge [1]. Its determination is valuable for membrane separations, to understand fouling [2–9], ageing [10–13] and rejection mechanisms [14,15]. It is therefore crucial to use characterisation techniques and develop optimised experimental protocols to determine the zeta potential of membranes reliably and accurately.

The zeta potential, as a surface charge indicator, is particularly useful for the characterization of layer-by-layer (LbL) modified membranes [16–20]. Its sensitivity to the surface charge sign makes it reliable to characterize the successively deposited layers of anionic and cationic polyelectrolytes. Layer-by-layer deposition of polyelectrolytes is a frequently used method to control electrostatic interactions, to understand the membrane fouling mechanisms [21] and to tune membrane separation performances [22]. Zeta potential cannot be measured directly and can only be calculated from experimentally measurable electrokinetic quantities such as the streaming potential or the streaming current [23–29]. Electrokinetic measurements are most often carried out in tangential mode in which an electrolyte solution is put in motion by a hydrostatic pressure gradient. Because of the tangential motion, this technique is aimed at providing information about the electrical properties of the outer surface of the membrane (skin layer).

However, it has been shown that a part of the streaming current generated by the hydrostatic pressure gradient is likely to flow through the porous layer(s) underneath the membrane surface [27]. This parasitic phenomenon can be taken into account by adding a contribution to the classical Smoluchowski equation as first proposed by Yaroshchuk and Luxbacher (2010) [27] and subsequently applied in a few studies [2,30,31].

In this study, we functionalized different types of membranes with polyelectrolytes with the aim of (i) showing that failure to take into account the electrokinetic leakage phenomenon could lead not only to significant quantitative errors in assessing the membrane surface zeta potential but also to qualitative errors when interpreting the experimental data and (ii) giving evidence that the parasitic contribution brought by the electrokinetic leakage phenomenon can also be used to obtain valuable complementary information on the phenomena occurring inside the pores of the modified membranes. The choice to focus this study on LbL assembled polyelectrolyte membranes was motivated by the inversion of sign of the surface charge expected when alternating layers of polycations and polyanions, but the conclusions drawn from this work can be generalised to any type of membrane functionalization.

2. Theoretical background

In order to achieve electrokinetic measurements, most often two flat membrane samples are placed facing each other and separated by a distance h_{ch} (gap height, Figure 1). The channel thus formed between the samples is filled with an electrolyte solution, which is further put into motion thanks to a pressure gradient. The solution therefore moves tangentially to the charged surfaces of the samples, carrying ions towards the low-pressure side [27,31]. As the solution contains an excess of counterions (to balance the surface charge of the samples), an electric current, called streaming current (I_s), is generated. If the thickness of the channel formed between the samples is much larger than the Debye length of the solution, the zeta potential (ζ) of the membrane surface can be calculated from streaming current measurements with the classical Smoluchowski equation (when applied to tangential electrokinetic measurements, it implicitly assumes dense and non-conducting samples):

$$I_s = \frac{W h_{ch} \varepsilon_0 \varepsilon_r \Delta P}{\eta L} \zeta \quad (1)$$

with,

W: channel width

L: channel length

ε_0: vacuum permittivity

ε_r: dielectric constant

η: viscosity

ΔP: pressure difference

It has been demonstrated that for porous membranes the classical Smoluchowski approach may break down [27] if a part of the streaming current is likely to flow through the porous layer(s) underneath the membrane surface (Figure 1). This parasitic phenomenon has been called electrokinetic leakage [2]. Describing the sample/channel/sample system as a parallel electrical circuit, Yaroshchuk and Luxbacher [27] derived the following equation as an alternative to the classical Smoluchowski equation (which implicitly assumes that the experimentally measured streaming current (I_s) does not flow elsewhere than in the channel formed by the two samples of membranes):

$$I_s = I_s^{ch} + 2I_s^{pore} = \frac{Wh_{ch}\varepsilon_0\varepsilon_r\Delta P}{\eta L}\zeta_{surf} + \frac{2Wh_{mb}^{eff}\varepsilon_0\varepsilon_r\Delta P}{\eta L}\zeta_{pore} \quad (2)$$

with,

I_s^{ch}: part of the streaming current circulating in the channel (i.e. along the membranes surfaces; see Fig. 1)

I_s^{pore}: part of the streaming current circulating in each sample (the term $2I_s^{pore}$ represents the electrokinetic leakage)

h_{mb}^{eff}: effective thickness in which the electrokinetic leakage occurs

ζ_{surf}: zeta potential of the membrane external surface

ζ_{pore}: zeta potential of the membrane pores.

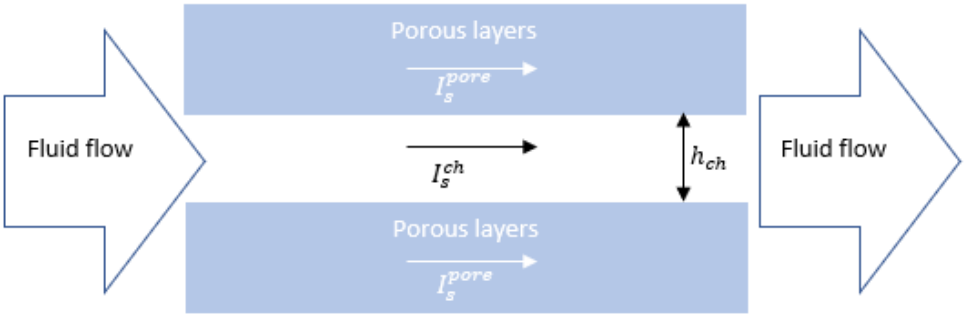

Figure 1: Possible pathways of the streaming current. The total streaming current $\boldsymbol{I_s}$ measured by an electrokinetic analyzer is equal to $\boldsymbol{I_s^{ch} + 2I_s^{pore}}$.

According to Eq. 2, the surface zeta potential (ζ_{surf}) can be determined by measuring the streaming current for different channel heights (h_{ch}). Indeed, by plotting the streaming current coefficient ($I_s/\Delta P$) as a function of h_{ch}, Eq. (2) predicts a linear variation and shows that ζ_{surf} can be obtained from the slope. As for ζ_{pore}, it can be inferred from the y-intercept provided that the effective height where the electrokinetic leakage occurs (h_{mb}^{eff}) is known, which requires measuring the electric conductance (G_{cell}) at different channel heights [27]:

$$G_{cell} = \frac{W}{L}\left(h_{ch}\lambda_0 + 2h_{mb}^{eff}\lambda_{mb}\right) \quad (3)$$

with,

λ_0: bulk conductivity

λ_{mb}: conductivity in the membrane pores

Eq. 3 can be further simplified if the membrane pores are much larger than the Debye length of the solution by assuming $\lambda_0 \approx \lambda_{mb}$. It should be noted, however, that in the case of pore size comparable to or smaller than the Debye length, this approximation would only lead to the determination of effective zeta potentials inside pores.

3. Experimental section

3.1 Chemicals

Poly(allylamine hydrochloride) (PAH; MW 15,000 g/mol), branched poly(ethyleneimine) (PEI; MW 800 g/mol) and poly(4-styrene sulfonic acid) solution (PSS; MW 75,000 g/mol; 18wt.% in H_2O) were purchased from Sigma-Aldrich. Their chemical structures are shown in Figure 2.

For the electrokinetic measurements and membrane modification, KCl (Fisher Scientific) and NaCl (Sigma-Aldrich) solutions were prepared with deionised water (resistivity: 18 MΩ.cm). The pH of electrolyte solutions was adjusted with HCl (Sigma-Aldrich) and KOH solutions (Fisher Chemical).

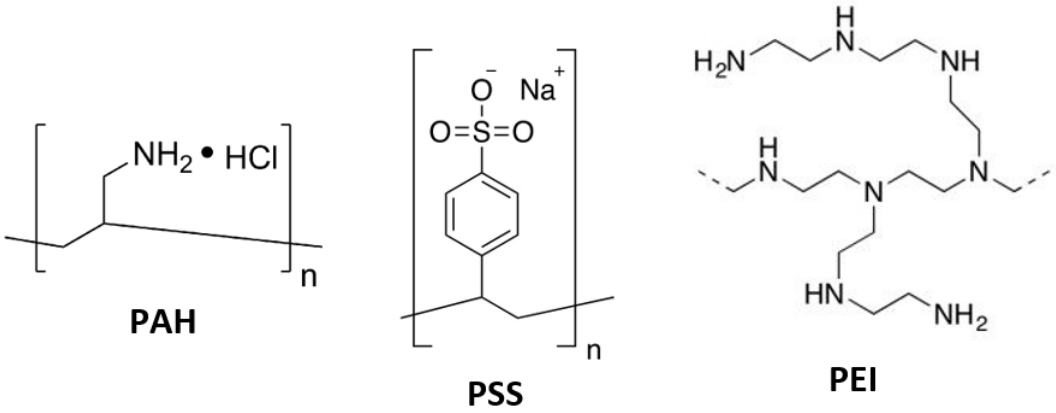

Figure 2: Chemical structure of the polyelectrolytes used in this work.

3.2 Membranes

Three flat-sheet membranes were used as substrates for polyelectrolyte deposition: NF270 nanofiltration semi-aromatic polyamide membrane (FilmTec^{TM}) with a molecular weight cut-

off (MWCO) of 400 Da, a regenerated cellulose (RC) microfiltration membrane (Sartorius) with an average pore diameter of 0.45 µm, and a polyvinyl chloride-silica (PVC-SiO_2) mixed matrix membrane (Amer Sil) with a 0.50 ±0.01 mm average thickness (Mitutoyo micrometer) and a bimodal pore structure (small pores in the range 0.02-0.1 µm, and larger ones between 1 and 2 µm [32–34]).

3.3 Layer-by-layer modification

The unmodified membranes were cut and fixed onto rectangular sample holders (L = 2 cm; W = 1 cm) using double-sided adhesive tape. Three different polyelectrolyte solutions containing 0.01 M NaCl were prepared for layer-by-layer surface modification (Table 1). First, the membrane sample was gently rinsed with deionised water for 1 min. The NF270, RC and PVC-SiO_2 membranes were then soaked in the PEI solution for 30, 15 and 1 min, respectively. The membranes were then rinsed again for 1 min. After the PEI deposition, one PSS/PAH bilayer was deposited on the membrane surface. The samples were contacted with the polyelectrolyte solution for 1 min, and then rinsed for 1 min. The pH of deposition of PEI and PSS (strong PE) solutions were not adjusted. For the PAH solution, the deposition pH was set to 3.7 to insure a full ionization of PAH chains [14].

Table 1: Polyelectrolyte type, pH and composition of the solutions used for LbL assembly.

Solution	pH	Polyelectrolyte concentration (M) [35]	NaCl concentration (M) [14,36]
PEI (+)	11.0	6.67×10^{-3}	0.01
PAH (+)	3.7	1.43×10^{-5}	0.01
PSS (-)	2.6	1.43×10^{-5}	0.01

3.4 Electrokinetic measurements

Electrokinetic measurements were conducted with a SurPass electrokinetic analyser (Anton Paar GmbH, Graz, Austria) equipped with an adjustable-gap cell. The streaming current was measured with Ag/AgCl electrodes by applying pressure ramps of 0.3 bar and periodically alternating the flow direction to limit electrode polarization. Electric conductance measurements were performed in alternative current mode under no flow conditions [37].

Before measurements, the membranes samples were soaked for at least 24 hours in a 10^{-3} M KCl solution. They were then attached to sample holders using double-sided adhesive tape (the sample support surface was gently wiped with a tissue paper to dry it sufficiently to ensure good

adhesion with the adhesive) and further inserted in the adjustable-gap cell. The KCl electrolyte solution (500 mL) was circulated between the polyelectrolyte membrane samples for 2.5 hours in order to remove the excess of loosely bound polyelectrolyte remaining on the surface after layer-by-layer modification [22,38] and to obtain a stable signal. Electrokinetic measurements were then performed at an average temperature of 22 ± 3 °C.

Each membrane was characterized according to two separate experimental protocols:

(i) The streaming current was measured for a fixed gap height and pH ranging from ~8 to ~3 (pH was adjusted by 0.05 M KOH and HCl solutions). Each time the pH was changed, the solution was circulated for about 20 minutes to allow the new solution to replace the previous one in the membrane pores and to equilibrate with the pore surface, before performing streaming current measurements. The zeta potential was further determined from the Smoluchowski equation (Eq. 1) and is denoted as apparent zeta potential in the following. This protocol is hereafter referred to as standard approach.

(ii) The streaming current and the electric cell conductance were measured at a fixed pH value for various gap heights ranging from ~100 µm to ~40 µm. The zeta potential was further determined by plotting the experimental streaming current coefficient (I_s/ΔP) and making use of Eq. 2. This protocol is hereafter referred to as advanced protocol.

The gap height (h_{ch}) was calculated from the hydrodynamic flow rate thanks to the Hagen-Poiseuille relation for parallelepipedic channels (Eq. 4), neglecting the contribution of the membrane pores to the total hydrodynamic volume flow rate (Q_v):

$$h_{ch} = \sqrt[3]{\frac{12\eta L Q_v}{W \Delta P}} \tag{4}$$

4. Results and discussion

4.1 Importance of the electrokinetic leakage phenomenon for the different membranes

Figure 3 shows the experimental streaming current coefficient (I_s/ΔP) measured at various channel heights for the three membranes under consideration.

As expected from Eq. 2, the streaming current coefficient varies linearly with the gap height for all three membranes. Negative slopes were obtained, meaning that the surface zeta-potentials of the unmodified membranes were negative (according to Eq. 2). Extrapolation of experimental data at zero gap height leads to non-zero values, which means that a non-zero current circulated through the membrane samples during measurements. The value of the electrokinetic leakage is therefore given by the value of the y-intercept. It depends on the structural properties (thickness, porosity, tortuosity) and surface chemistry (hydrophobicity/hydrophilicity, surface charge density) of the membrane but also on the geometry of the measuring cell as the sample cross-section may be more or less exposed to the hydrodynamic flow depending on the design of the measuring cell [31]. Considering arbitrarily the streaming current coefficient measured for a gap height of 100 µm as a reference value, the contribution of the electrokinetic leakage to the total measured current was found relatively negligible (about 10%) for the NF270 nanofiltration membrane, much larger (41%) for the microfiltration RC membrane and quite dominant (90%) for the thick and coarse-porous PVC-SiO_2 membrane.

The contribution of the electrokinetic leakage to the measured current obviously depends on the distance set between the samples, since the current flowing in the channel (I_s^{ch}; see Figure 1) depends on h_{ch}, whereas the current flowing in the samples (I_s^{pore}) is independent of h_{ch}. Consequently, when the electrokinetic leakage is not negligible, the value of the apparent zeta potential deduced from the Smoluchowski equation (Eq. 1) is (i) incorrect and (ii) dependent on the distance set between the membrane samples. It is illustrated in Figure 4 which shows the pH dependence of the apparent zeta potential of the RC membrane for two different channel heights (103 ± 2 µm and 58 ± 2 µm). It is found that the apparent zeta potential deduced from the standard approach becomes more negative when decreasing the distance between samples because the contribution of the electrokinetic leakage to the total current measured by the electrokinetic analyzer increases with decreasing h_{ch}. We believe that the failure to account for the electrokinetic leakage in streaming current and streaming potential measurements may partly explain the significant discrepancies in zeta potentials reported in the literature for similar membranes (as stated above, the magnitude of the electrokinetic leakage for a given membrane depends on the type of measuring cell and thus on the electrokinetic analyzer).

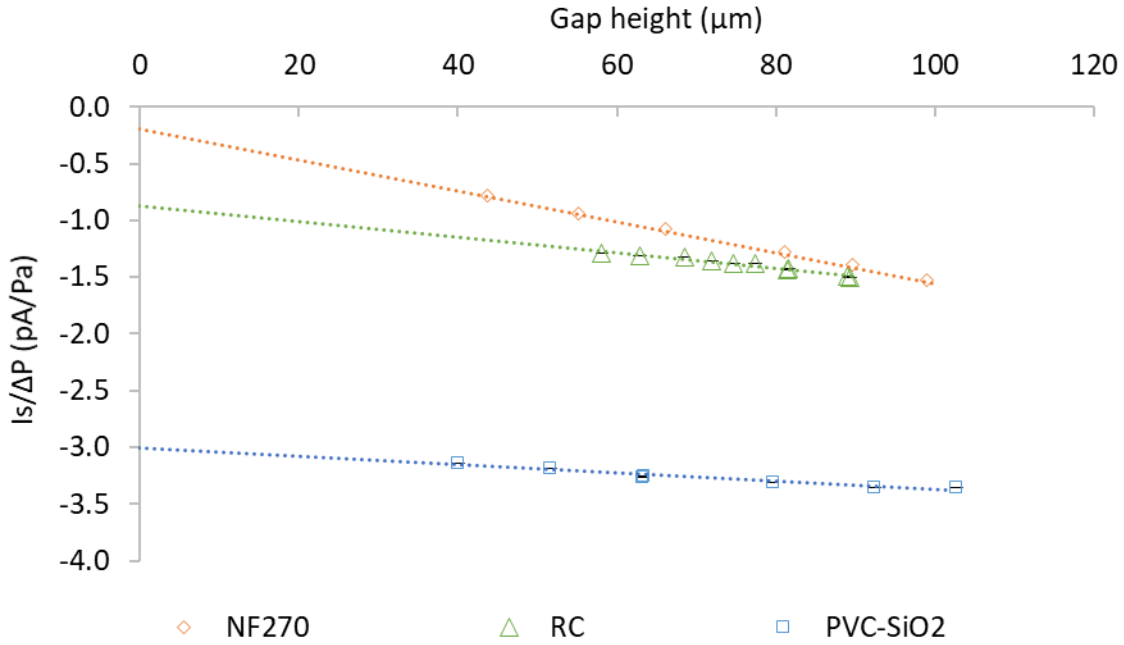

Figure 3: Streaming current coefficient (I_s/ΔP) of the unmodified NF270, RC and PVC-SiO_2 membranes versus gap height; Solution: 0.001 M KCl at pH 5.60 ± 0.05.

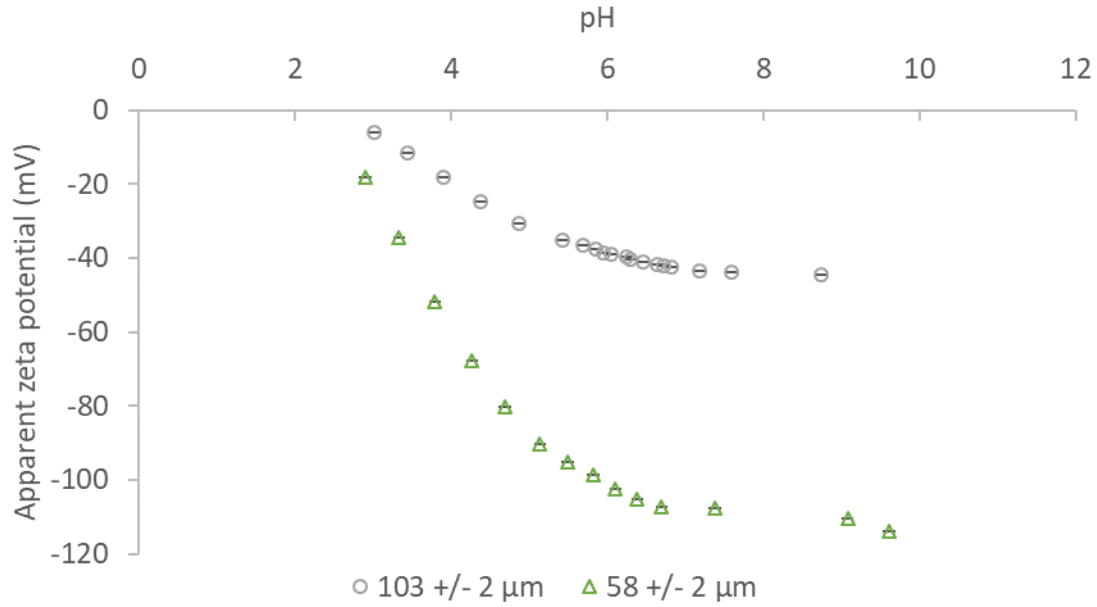

Figure 4: Apparent zeta potential of the RC unmodified membrane (determined from the Smoluchowski equation) versus pH for two gap heights (h_{ch} = 103 ± 2 µm and 58 ± 2 µm); Solution: 0.001 M KCl.

A simple method for checking whether a membrane is prone to electrokinetic leakage is to perform two successive streaming current measurements, changing only the gap height between the samples, and compare the values of the zeta potential obtained by the Smoluchowski

equation. Indeed, if different values are obtained, this means that electrokinetic leakage in the membranes is not negligible and that a reliable and accurate determination of the zeta potential requires following the advanced protocol and using Eq. 2.

4.2 Surface functionalization

Electrokinetic measurements were then conducted on unmodified and layer-by-layer modified membranes. Figure 5 shows the pH dependence of the apparent zeta potential (calculated with Eq. 1) of the unmodified and layer-by-layer modified PVC-SiO_2 membranes.

The apparent zeta potential was found less negative after membrane modification. For instance, at pH 5.5, the apparent zeta potential increased from -89.8 mV for the unmodified membrane to -49.4 mV for the PEI/PSS/PAH modified one. The conclusion that would be drawn by following this standard approach is that the surface of the modified membrane remains negatively charged, which is not expected for a cationic polyelectrolyte (PAH) terminated membrane..

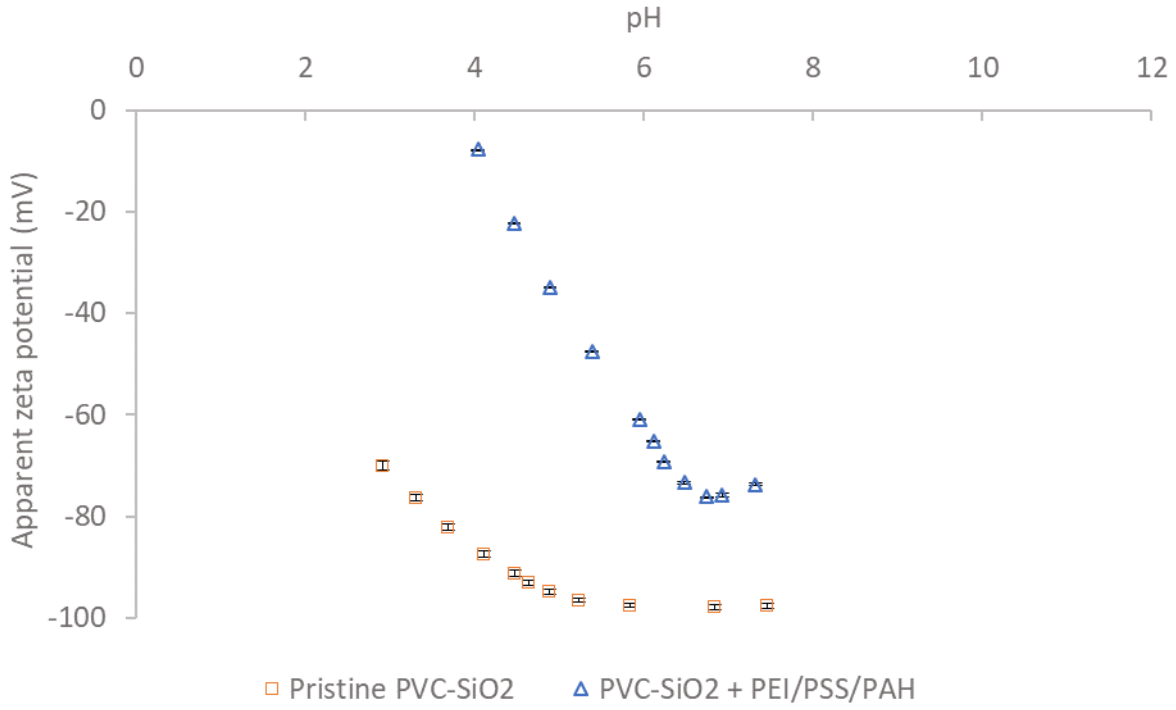

Figure 5: Apparent zeta potential of the unmodified and PEI/PSS/PAH modified PVC-SiO_2 membranes versus pH for $\boldsymbol{h_{ch}} = 98 \pm 1$ µm; Solution: 0.001 M KCl.

However, Figure 6 provides evidence that the electrokinetic leakage phenomenon is actually responsible for this apparent contradiction. Indeed, by plotting the streaming current coefficient versus the gap height, a change in the sign of the slope is observed, from negative for the

unmodified membrane ($-3.38 \times 10^{-15}\ A.Pa^{-1}.\mu m^{-1}$) to positive for the PEI/PSS/PAH modified membrane ($+3.96 \times 10^{-15}\ A.Pa^{-1}.\mu m^{-1}$). As shown by Eq. 2, the slope has the same sign as the surface zeta potential. The advanced protocol thus makes it possible to highlight the positive surface charge density of the modified membrane terminated by the PAH layer.

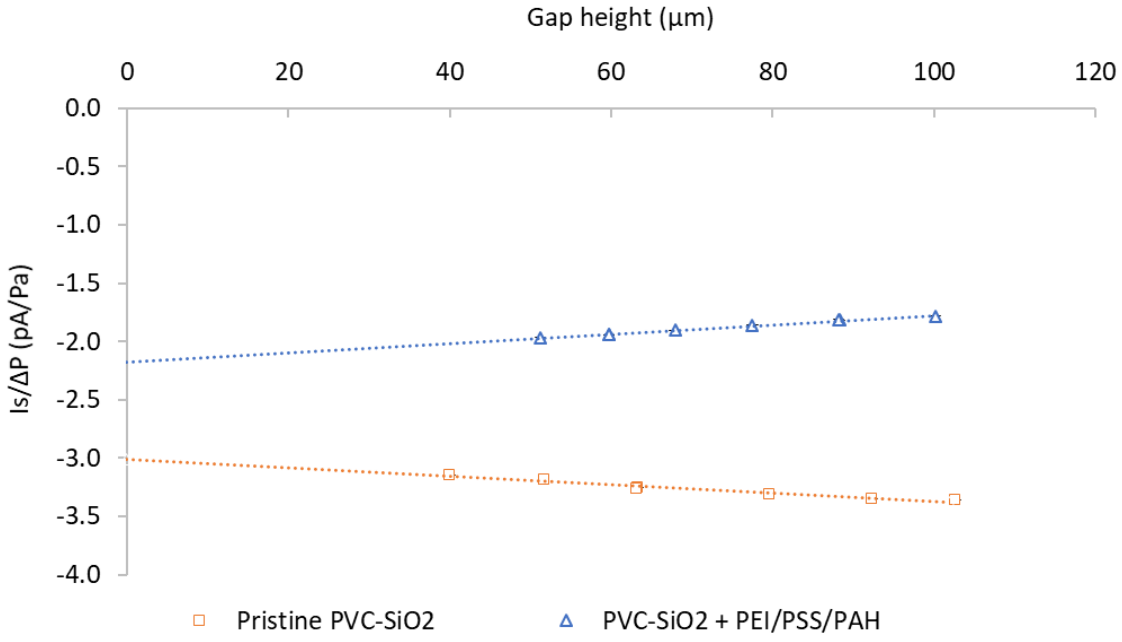

Figure 6: Streaming current coefficient ($\boldsymbol{I_s}$/ΔP) of the unmodified and PEI/PSS/PAH modified PVC-SiO_2 membranes versus gap height; Solution: 0.001 M KCl at pH 5.60 ± 0.05.

Figure 7 shows the comparison of the zeta potentials determined at pH 5.60 for the unmodified and modified PVC-SiO_2 membranes following the standard approach and the advanced protocol (i.e. considering the electrokinetic leakage phenomenon). For the unmodified membrane, a 89% difference was observed between the surface zeta potentials determined from both protocols, which results from the strong electrokinetic leakage occurring through the PVC-SiO_2 membrane (see section 4.1). For the PEI/PSS/PAH modified membrane, the advanced protocol led a positive surface zeta potential of +11.1 mV (consistent with the cationic polyelectrolyte deposition on the membrane surface) while the standard approach led to a negative apparent zeta potential. The reason is that the positive streaming current generated along the membrane surface by the PAH layer is overcompensated by the negative current associated with the electrokinetic leakage occurring in the samples, so that the total current measured by the electrokinetic analyzer is negative, leading to a qualitatively wrong

interpretation when following the standard approach (based on the Smoluchowski equation) in which the electrokinetic leakage is not subtracted from the total measured current.

These results demonstrate that not considering the electrokinetic leakage phenomenon can not only induce quantitative errors on the value of the zeta potential but can also lead to a qualitatively wrong interpretation of the raw experimental data.

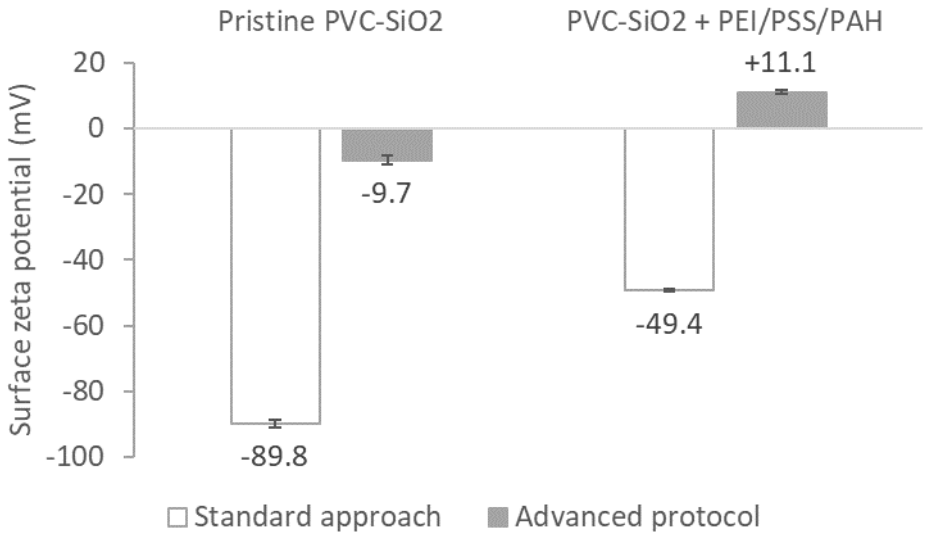

Figure 7: Surface zeta potential of PVC-SiO_2 calculated with the standard approach and the advanced protocol; Solution: 0.001 M KCl at pH 5.60 ± 0.05.

The same protocol was applied to the RC membrane, and led to similar results and conclusion (see Figure S1 in the supporting information).

However, no significant difference was observed when comparing the standard approach and the advanced protocol for the NF270 membrane (Figure 8). Indeed, both approaches led to similar conclusions both quantitatively and qualitatively. Notably, the standard approach was found able to highlight the positive charge density on the surface of the NF270 membrane after PEI/PSS/PAH layer-by-layer modification. The reason for this is that the electrokinetic leakage was found to be very low for the NF270 membrane (see section 4.1) and thus the standard approach based on the Smoluchowski equation is reliable for this membrane.

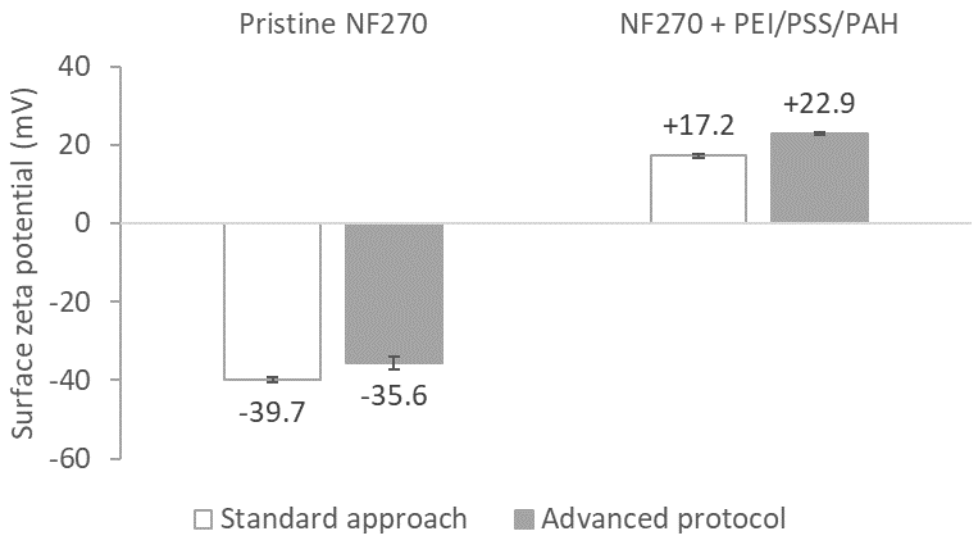

Figure 8: Surface zeta potential of the NF270 membrane calculated with the standard approach and the advanced protocol; Solution: 0.001 M KCl at pH 5.60 ± 0.05.

4.3 Extracting information from the electrokinetic leakage

So far, we have shown that the advanced protocol based on the measurement of the streaming current at different gap heights and Eq. 2 allows to correctly interpret the data of electrokinetic experiments and to determine a reliable value of the membrane surface zeta potential. In the last part of this work, we wished to demonstrate that the electrokinetic leakage phenomenon, considered up to this point as a signal interfering with the electrokinetic measurements, can be used to extract additional information on the membrane functionalization process.

Figure 9 shows the experimental streaming current coefficient ($I_s/\Delta P$) measured for the NF270 membrane at various channel heights, before and after PEI/PSS/PAH layer-by-layer modification. As stated above, the change in sign of the slope observed after modification of the membrane by PEI/PSS/PAH deposition indicates the reversal of the sign of the surface charge density (from negative to positive) and thus the successful membrane surface modification.

Figure 9 also shows that the y-intercept remained similar before and after PEI/PSS/PAH modification, which indicates that the electrokinetic leakage was not altered after the modification of the NF270 membrane. In other words, the polyelectrolytes were deposited onto the membrane surface without penetrating into the membrane. It is worth noting that this result can be interpreted in light of the concept of pore-dominated and layer-dominated regimes first introduced by de Grooth et al. [39]. The pore-dominated regime occurs if the polyelectrolyte layers are formed inside the pores of the support. After the deposition of a certain number of

layers, a transition occurs leading to the layer-dominated regime where additional polyelectrolyte layers are formed on top of the support [40]. The results shown in Figure 9 therefore demonstrate that, in the case of the NF270 membrane, the layer-dominated regime was reached from the first adsorbed layer (PEI) since the intensity of the electrokinetic leakage did not vary after polyelectrolyte adsorption. This result is consistent with the narrow pores of the NF270 nanofiltration membrane.

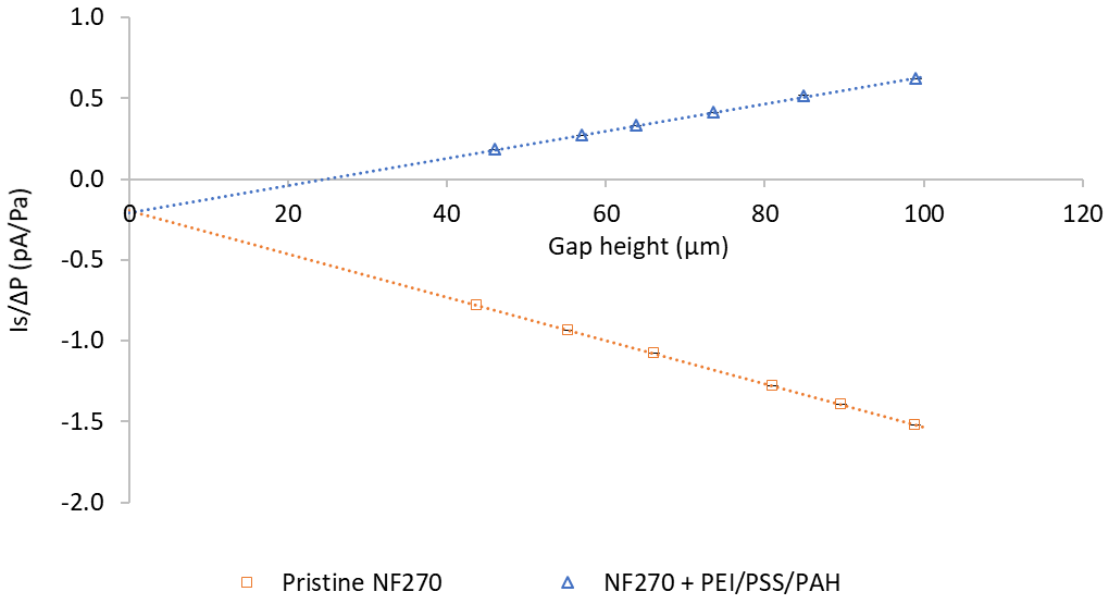

Figure 9: Streaming current coefficient (I_s/ΔP) of the unmodified and PEI/PSS/PAH modified NF270 membranes versus gap height; Solution: 0.001 M KCl at pH 5.60 ± 0.05.

Unlike the results obtained with the NF270 membrane, a decrease of about 25% in the electrokinetic leakage was observed after modification of the RC microfiltration membrane by PEI/PSS/PAH deposition (see Figure 10). The electrokinetic leakage alteration indicates that a certain amount of polyelectrolytes entered the RC membrane and adsorbed inside pores. Similar results were obtained with the PVC-SiO_2 membrane (see Figure 6). The fact that the intensity of the electrokinetic leakage varies after polyelectrolyte adsorption is the signature of the pore-dominated regime. Interestingly, the sign of the electrokinetic leakage remained negative after adsorption of the terminating polycation layer, which means that the polyelectrolytes deposited in the pores of the support did not cover all the porosity accessible to electrokinetic leakage.

de Grooth et al. showed that the distinction between pore-dominated and layer-dominated regimes could be made on the basis of (i) the different mechanisms of membrane rejections, the rejections being mainly steric in the case of the pore-dominated regime and governed by

Donnan exclusion for the layer-dominated regime and (ii) the flip of the so-called odd-even effect on membrane permeability [39]. The advanced electrokinetic protocol used in the present work provides an alternative method since the pore-dominated regime can be associated with a variation of the electrokinetic leakage intensity with the number of deposited layers whereas an electrokinetic leakage independent of the number of deposited layers can be associated with the layer-dominated regime.

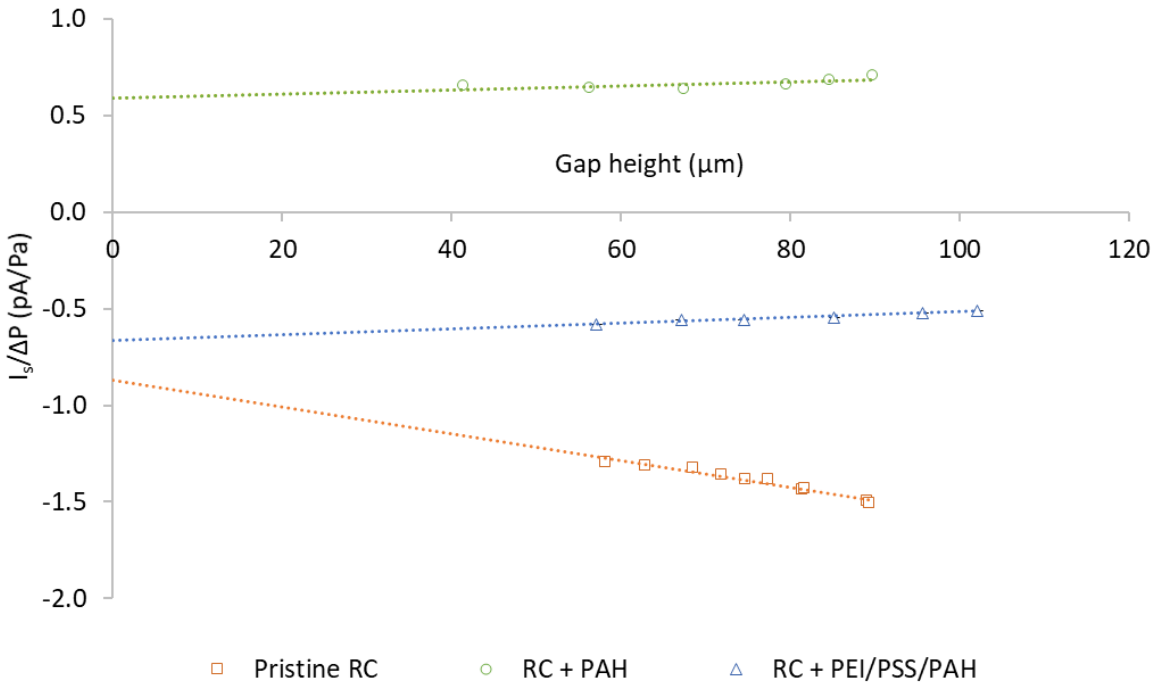

Figure 10: Streaming current coefficient ($\boldsymbol{I_s}$/ΔP) of the unmodified, PAH modified and PEI/PSS/PAH modified RC membranes versus gap height; Solution: 0.001 M KCl at pH 5.40 ± 0.05.

As shown in Figure 10, the modification of the RC membrane by a single layer of PAH (without prior deposition of PEI and PSS) resulted in a change of sign of the electrokinetic leakage. This result indicates a significant adsorption of the polycation inside the RC membrane pores leading to charge inversion inside the pores. With the help of additional measurements of the cell electrical conductance versus the gap height and Eqs. 2 and 3 (using the approximation $\lambda_0 \approx \lambda_{mb}$ in Eq. 3, which was reasonable since the pore size of the RC microfiltration membrane was much larger than the Debye length of the measurement solution, i.e. around 10 nm for a millimolar solution of a mono-monovalent electrolyte), the surface and inner zeta potentials (ζ_{surf} and ζ_{pore}, respectively) of the unmodified and modified RC membranes were determined

(Figure 11). As expected, similar values of ζ_{surf} and ζ_{pore} were obtained for the unmodified membrane. After modification, the surface zeta potential of the RC membrane increased from -18.5 mV to +2.8 mV and +4.0 mV (at pH = 5.40) for the two modified membranes terminated by a PAH layer. The impact of the PEI layer is highlighted by comparing ζ_{pore} for the membranes modified by PEI/PSS/PAH (-10.0 mV) and PAH only (+9.9 mV). It has been reported that branched PEI tends to form a web onto solid surfaces [41–43] and thus it hinders the subsequent penetration of PSS and PAH polyelectrolytes inside the RC membrane. These results suggest that the phenomenon of electrokinetic leakage could be an additional tool for providing insight into the complex mechanisms of deposition of polyelectrolyte layers in the membrane pores before reaching the layer-dominated regime [38].

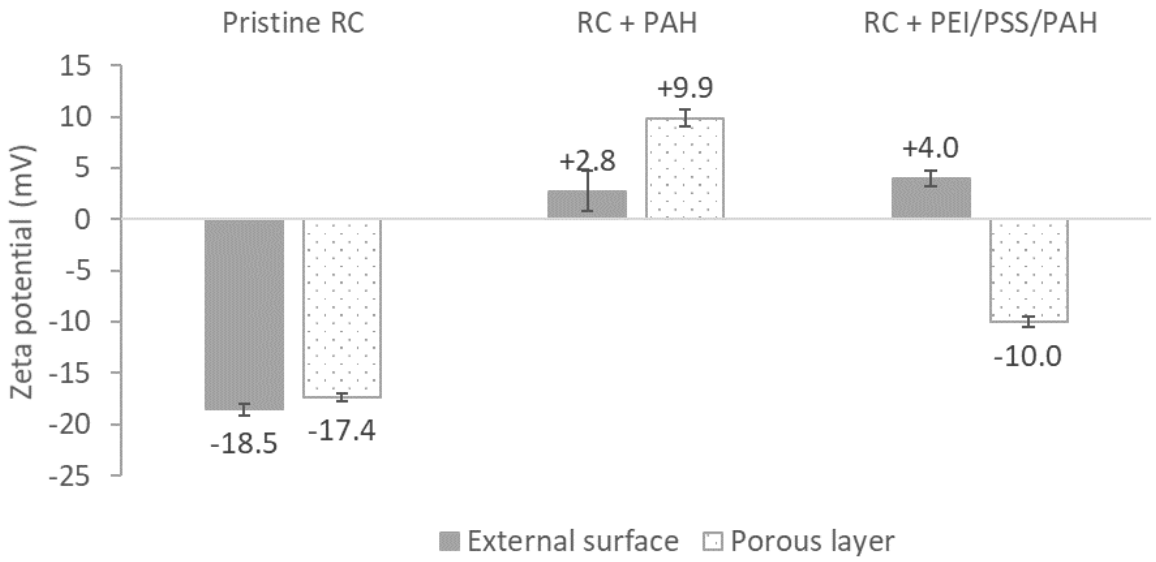

Figure 11: External surface and pore surface zeta potentials of the unmodified, PAH and PEI/PSS/PAH modified RC membranes calculated with the advanced protocol; Solution: 0.001 M KCl at pH 5.40 ± 0.05.

As a final remark, it is worthwhile that LbL assembled polyelectrolyte membranes are often processed as hollow fiber membranes [39,44], where the common way to determine their zeta potential is to prepare a small module filled with a resin on the outside of the membrane so that the measuring solution cannot permeate the membrane. It must be stressed, however, that the use of such modules does not prevent the electrokinetic leakage through the membrane pores as demonstrated by Efligenir et al. [45]. It should be kept in mind, however, that the advanced protocol followed in the present study relies on a modification of the geometry of the channel

formed by the samples analyzed, which is not possible with a hollow fiber membrane since in this case the channel geometry is fixed by the internal diameter of the membrane.

5. Conclusion

When tangential streaming current (or streaming potential) measurements are performed with membranes, a part of the current measured by the electrokinetic analyzer may come from a parasitic contribution occurring through the porosity of the membrane samples. This phenomenon, known as electrokinetic leakage, can lead to misinterpretations of the electrokinetic data. In this work, it was shown that the characterization by a standard approach (i.e. based on the classical Smoluchowski equation) of layer-by-layer modified polyelectrolytes membranes can be flawed not only quantitatively but also qualitatively if the phenomenon of electrokinetic leakage is not considered in the interpretation of the raw data. A rigorous and reliable characterization requires the use of an advanced characterization protocol based on the measurement of the streaming current by varying the spacing between the two samples needed for the measurements. This advanced protocol was applied to three types of membranes of different nature and structure (a polyamide nanofiltration membrane and two macroporous membranes, one made of regenerated cellulose and the other with a mixed PVC-SiO_2 matrix) which were then modified with polyelectrolytes (PAH or PEI/PSS/PAH). It was shown that the advanced protocol accounting for the electrokinetic leakage phenomenon allowed a reliable and accurate characterization of the various membranes. Moreover, the analysis of the electrokinetic leakage before and after membrane modification provided information on whether the polyelectrolytes were deposited only on the membrane surface or whether they were able to enter the membrane and adsorb onto its pores. Electrokinetic characterization rigorously performed using the advanced protocol can thus not only demonstrate the success of membrane surface modification but also provide insightful information on polyelectrolyte penetration. The electrokinetic leakage phenomenon could also be used to monitor the transition between the so-called pore-dominated and layer-dominated regimes as its intensity is expected to vary with the number of polyelectrolytes layers in the pore-dominated regime, but be independent of the number of deposited layers in the layer-dominated regime. Importantly, the conclusions drawn from this work are not limited to LbL assembled polyelectrolyte membranes but can be generalised to any type of membrane functionalization.

References

[1] P. Leroy, A. Maineult, S. Li, J. Vinogradov, The zeta potential of quartz. Surface complexation modelling to elucidate high salinity measurements, Colloids Surf. Physicochem. Eng. Asp. 650 (2022) 129507. https://doi.org/10.1016/j.colsurfa.2022.129507.

[2] C. Rouquié, S. Liu, M. Rabiller-Baudry, A. Riaublanc, M. Frappart, E. Couallier, A. Szymczyk, Electrokinetic leakage as a tool to probe internal fouling in MF and UF membranes, J. Membr. Sci. 599 (2020) 117707. https://doi.org/10.1016/j.memsci.2019.117707.

[3] E.M.V. Hoek, M. Elimelech, Cake-Enhanced Concentration Polarization: A New Fouling Mechanism for Salt-Rejecting Membranes, Environ. Sci. Technol. 37 (2003) 5581–5588. https://doi.org/10.1021/es0262636.

[4] T.O. Mahlangu, E.M.V. Hoek, B.B. Mamba, A.R.D. Verliefde, Influence of organic, colloidal and combined fouling on NF rejection of NaCl and carbamazepine: Role of solute–foulant–membrane interactions and cake-enhanced concentration polarisation, J. Membr. Sci. 471 (2014) 35–46. https://doi.org/10.1016/j.memsci.2014.07.065.

[5] M.-S. Chun, H. Il Cho, I.K. Song, Electrokinetic behavior of membrane zeta potential during the filtration of colloidal suspensions, Desalination. 148 (2002) 363–368. https://doi.org/10.1016/S0011-9164(02)00731-2.

[6] N.D. Lawrence, J.M. Perera, M. Iyer, M.W. Hickey, G.W. Stevens, The use of streaming potential measurements to study the fouling and cleaning of ultrafiltration membranes, Sep. Purif. Technol. 48 (2006) 106–112. https://doi.org/10.1016/j.seppur.2005.07.009.

[7] A.R.D. Verliefde, E.R. Cornelissen, S.G.J. Heijman, I. Petrinic, T. Luxbacher, G.L. Amy, B. Van der Bruggen, J.C. van Dijk, Influence of membrane fouling by (pretreated) surface water on rejection of pharmaceutically active compounds (PhACs) by nanofiltration membranes, J. Membr. Sci. 330 (2009) 90–103. https://doi.org/10.1016/j.memsci.2008.12.039.

[8] B. Teychene, P. Loulergue, C. Guigui, C. Cabassud, Development and use of a novel method for in line characterisation of fouling layers electrokinetic properties and for fouling monitoring, J. Membr. Sci. 370 (2011) 45–57. https://doi.org/10.1016/j.memsci.2010.12.014.

[9] Y. Lanteri, P. Fievet, C. Magnenet, S. Déon, A. Szymczyk, Electrokinetic characterisation of particle deposits from streaming potential coupled with permeate flux measurements during dead-end filtration, J. Membr. Sci. 378 (2011) 224–232. https://doi.org/10.1016/j.memsci.2011.05.002.

[10] E. Gaudichet-Maurin, F. Thominette, Ageing of polysulfone ultrafiltration membranes in contact with bleach solutions, J. Membr. Sci. 282 (2006) 198–204. https://doi.org/10.1016/j.memsci.2006.05.023.

[11] Y. Hanafi, P. Loulergue, S. Ababou-Girard, C. Meriadec, M. Rabiller-Baudry, K. Baddari, A. Szymczyk, Electrokinetic analysis of PES/PVP membranes aged by sodium hypochlorite solutions at different pH, J. Membr. Sci. 501 (2016) 24–32. https://doi.org/10.1016/j.memsci.2015.11.041.

[12] V.T. Do, C.Y. Tang, M. Reinhard, J.O. Leckie, Degradation of Polyamide Nanofiltration and Reverse Osmosis Membranes by Hypochlorite, Environ. Sci. Technol. 46 (2012) 852–859. https://doi.org/10.1021/es203090y.

[13] B. Pellegrin, F. Mezzari, Y. Hanafi, A. Szymczyk, J.-C. Remigy, C. Causserand, Filtration performance and pore size distribution of hypochlorite aged PES/PVP ultrafiltration membranes, J. Membr. Sci. 474 (2015) 175–186. https://doi.org/10.1016/j.memsci.2014.09.028.

[14] A.-N.D. Egueh, B. Lakard, P. Fievet, S. Lakard, C. Buron, Charge properties of membranes modified by multilayer polyelectrolyte adsorption, J. Colloid Interface Sci. 344 (2010) 221–227. https://doi.org/10.1016/j.jcis.2009.12.033.

[15] C. Labbez, P. Fievet, F. Thomas, A. Szymczyk, A. Vidonne, A. Foissy, P. Pagetti, Evaluation of the "DSPM" model on a titania membrane: measurements of charged and uncharged solute retention, electrokinetic charge, pore size, and water permeability, J. Colloid Interface Sci. 262 (2003) 200–211. https://doi.org/10.1016/S0021-9797(02)00245-X.
[16] T. Jimbo, M. Higa, N. Minoura, A. Tanioka, Surface Characterization of Poly(acrylonitrile) Membranes Graft-Polymerized with Ionic Monomers As Revealed by ζ Potential Measurement, Macromolecules. 31 (1998) 1277–1284. https://doi.org/10.1021/ma970692k.
[17] D. Scheepers, J. de Keizer, Z. Borneman, K. Nijmeijer, The pH as a tool to tailor the performance of symmetric and asymmetric layer-by-layer nanofiltration membranes, J. Membr. Sci. 670 (2023) 121320. https://doi.org/10.1016/j.memsci.2022.121320.
[18] B.A. Russell, B. Jachimska, Y. Chen, Polyallylamine hydrochloride coating enhances the fluorescence emission of Human Serum Albumin encapsulated gold nanoclusters, J. Photochem. Photobiol. B. 187 (2018) 131–135. https://doi.org/10.1016/j.jphotobiol.2018.08.018.
[19] R. Malaisamy, A. Talla-Nwafo, K.L. Jones, Polyelectrolyte modification of nanofiltration membrane for selective removal of monovalent anions, Sep. Purif. Technol. 77 (2011) 367–374. https://doi.org/10.1016/j.seppur.2011.01.005.
[20] J. Saqib, I.H. Aljundi, Membrane fouling and modification using surface treatment and layer-by-layer assembly of polyelectrolytes: State-of-the-art review, J. Water Process Eng. 11 (2016) 68–87. https://doi.org/10.1016/j.jwpe.2016.03.009.
[21] D. Breite, M. Went, A. Prager, A. Schulze, The critical zeta potential of polymer membranes: how electrolytes impact membrane fouling, RSC Adv. 6 (2016) 98180–98189. https://doi.org/10.1039/C6RA19239D.
[22] N. Joseph, P. Ahmadiannamini, R. Hoogenboom, I.F. J. Vankelecom, Layer-by-layer preparation of polyelectrolyte multilayer membranes for separation, Polym. Chem. 5 (2014) 1817–1831. https://doi.org/10.1039/C3PY01262J.
[23] T. Luxbacher, Electrokinetic characterization of flat sheet membranes by streaming current measurement, Desalination. 199 (2006) 376–377. https://doi.org/10.1016/j.desal.2006.03.085.
[24] A. Szymczyk, C. Labbez, P. Fievet, B. Aoubiza, C. Simon, Streaming potential through multilayer membranes, AIChE J. 47 (2001) 2349–2358. https://doi.org/10.1002/aic.690471019.
[25] P. Fievet, M. Sbaï, A. Szymczyk, C. Magnenet, C. Labbez, A. Vidonne, A New Tangential Streaming Potential Setup for the Electrokinetic Characterization of Tubular Membranes, Sep. Sci. Technol. 39 (2004) 2931–2949. https://doi.org/10.1081/SS-200028652.
[26] A. Szymczyk, N. Fatin-Rouge, P. Fievet, Tangential streaming potential as a tool in modeling of ion transport through nanoporous membranes, J. Colloid Interface Sci. 309 (2007) 245–252. https://doi.org/10.1016/j.jcis.2007.02.005.
[27] A. Yaroshchuk, T. Luxbacher, Interpretation of Electrokinetic Measurements with Porous Films: Role of Electric Conductance and Streaming Current within Porous Structure, Langmuir. 26 (2010) 10882–10889. https://doi.org/10.1021/la100777z.
[28] A. Yaroshchuk, V. Ribitsch, Role of Channel Wall Conductance in the Determination of ζ-Potential from Electrokinetic Measurements, Langmuir. 18 (2002) 2036–2038. https://doi.org/10.1021/la015557m.
[29] E. Idil Mouhoumed, A. Szymczyk, A. Schäfer, L. Paugam, Y.H. La, Physico-chemical characterization of polyamide NF/RO membranes: Insight from streaming current measurements, J. Membr. Sci. 461 (2014) 130–138. https://doi.org/10.1016/j.memsci.2014.03.025.

[30] S. Déon, P. Fievet, C. Osman Doubad, Tangential streaming potential/current measurements for the characterization of composite membranes, J. Membr. Sci. 423–424 (2012) 413–421. https://doi.org/10.1016/j.memsci.2012.08.038.
[31] A. Szymczyk, Y.I. Dirir, M. Picot, I. Nicolas, F. Barrière, Advanced electrokinetic characterization of composite porous membranes, J. Membr. Sci. 429 (2013) 44–51. https://doi.org/10.1016/j.memsci.2012.11.076.
[32] L. Marbelia, M.R. Bilad, N. Bertels, C. Laine, I.F.J. Vankelecom, Ribbed PVC–silica mixed matrix membranes for membrane bioreactors, J. Membr. Sci. 498 (2016) 315–323. https://doi.org/10.1016/j.memsci.2015.10.017.
[33] V. Toniazzo, New separators for industrial and specialty lead acid batteries, J. Power Sources. 107 (2002) 211–216. https://doi.org/10.1016/S0378-7753(01)01073-4.
[34] M.R. Bilad, L. Marbelia, C. Laine, I.F.J. Vankelecom, A PVC–silica mixed-matrix membrane (MMM) as novel type of membrane bioreactor (MBR) membrane, J. Membr. Sci. 493 (2015) 19–27. https://doi.org/10.1016/j.memsci.2015.05.074.
[35] J. Wang, Y. Ren, H. Zhang, J. Luo, J.M. Woodley, Y. Wan, Targeted modification of polyamide nanofiltration membrane for efficient separation of monosaccharides and monovalent salt, J. Membr. Sci. 628 (2021) 119250. https://doi.org/10.1016/j.memsci.2021.119250.
[36] B. Jachimska, T. Jasiński, P. Warszyński, Z. Adamczyk, Conformations of poly(allylamine hydrochloride) in electrolyte solutions: Experimental measurements and theoretical modeling, Colloids Surf. Physicochem. Eng. Asp. 355 (2010) 7–15. https://doi.org/10.1016/j.colsurfa.2009.11.012.
[37] Y. Sedkaoui, A. Szymczyk, H. Lounici, O. Arous, A new lateral method for characterizing the electrical conductivity of ion-exchange membranes, J. Membr. Sci. 507 (2016) 34–42. https://doi.org/10.1016/j.memsci.2016.02.003.
[38] M.A. Junker, W.M. de Vos, J. de Grooth, R.G.H. Lammertink, Relating uncharged solute retention of polyelectrolyte multilayer nanofiltration membranes to effective structural properties, J. Membr. Sci. 668 (2023) 121164. https://doi.org/10.1016/j.memsci.2022.121164.
[39] J. de Grooth, R. Oborný, J. Potreck, K. Nijmeijer, W.M. de Vos, The role of ionic strength and odd–even effects on the properties of polyelectrolyte multilayer nanofiltration membranes, J. Membr. Sci. 475 (2015) 311–319. https://doi.org/10.1016/j.memsci.2014.10.044.
[40] D. Scheepers, B. Chatillon, Z. Borneman, K. Nijmeijer, Influence of charge density and ionic strength on diallyldimethylammonium chloride (DADMAC)-based polyelectrolyte multilayer membrane formation, J. Membr. Sci. 617 (2021) 118619. https://doi.org/10.1016/j.memsci.2020.118619.
[41] M. Kolasińska, R. Krastev, P. Warszyński, Characteristics of polyelectrolyte multilayers: Effect of PEI anchoring layer and posttreatment after deposition, J. Colloid Interface Sci. 305 (2007) 46–56. https://doi.org/10.1016/j.jcis.2006.09.035.
[42] Y. Kapilov-Buchman, E. Lellouche, S. Michaeli, J.-P. Lellouche, Unique Surface Modification of Silica Nanoparticles with Polyethylenimine (PEI) for siRNA Delivery Using Cerium Cation Coordination Chemistry, Bioconjug. Chem. 26 (2015) 880–889. https://doi.org/10.1021/acs.bioconjchem.5b00100.
[43] Z. Zhao, H. Kantamneni, S. He, S. Pelka, A.S. Venkataraman, M. Kwon, S.K. Libutti, M. Pierce, P.V. Moghe, V. Ganapathy, M.C. Tan, Surface-Modified Shortwave-Infrared-Emitting Nanophotonic Reporters for Gene-Therapy Applications, ACS Biomater. Sci. Eng. 4 (2018) 2350–2363. https://doi.org/10.1021/acsbiomaterials.8b00378.
[44] J. de Grooth, B. Haakmeester, C. Wever, J. Potreck, W.M. de Vos, K. Nijmeijer, Long term physical and chemical stability of polyelectrolyte multilayer membranes, J. Membr. Sci. 489 (2015) 153–159. https://doi.org/10.1016/j.memsci.2015.04.031.

[45] A. Efligenir, P. Fievet, S. Déon, P. Sauvade, Tangential electrokinetic characterization of hollow fiber membranes: Effects of external solution on cell electric conductance and streaming current, J. Membr. Sci. 496 (2015) 293–300. https://doi.org/10.1016/j.memsci.2015.09.002.